Synthesis and Properties of Polyetherketone-*block*-Polybenzobisthiazole-*block*-Polyetherketone ABA Triblock Copolymers

Jong-Beom Baek*,† and Loon-Seng Tan*,‡

School of Chemical Engineering, Chungbuk National University, Cheongju, Chungbuk, 361-763 South Korea, and Nanostructured & Biological Materials Branch, Materials & Manufacturing Directorate, AFRL/RXBP, Air Force Research Laboratory, Wright-Patterson Air Force Base, Dayton, Ohio 45433-7750

Received August 6, 2007; Revised Manuscript Received December 26, 2007

ABSTRACT: As an approach to rigid-rod molecular composites, a series of PEK-*b*-PBZT-*b*-PEK ABA triblock copolymers were synthesized. Three different types of polyetherketones (PEKs) as coil A-block units and the carboxylic acid-terminated polybenzobisthiazoles (PBZTs) with two different molecular weights as rigid-rod B-block units were utilized to afford the targeted ABA triblock copolymers. The resulting triblock copolymers were insoluble in common polar aprotic solvents such as *N*-methylpyrrolidinone, dimethylformamide, dimethylacetamide, and dimethyl sulfoxide but showed greatly improved solubility in strong acids such as trifluoroacetic acid, methanesulfonic acid (MSA), trifluoromethanesulfonic acid, and sulfuric acid. Good quality films could be cast from solutions. Alternatively, we could also process these copolymers by the compression molding technique. The block copolymer samples were simply heated above the transition temperatures of the coil components and pressed into articles with desired shapes. The wide-angle X-ray diffraction study of the selected solution-cast film exhibited a long-range ordering, which is indicative of microphase separation. This was further confirmed by the results from small-angle X-ray diffraction, scanning electron microscopy, and transmission electron microscopy. In addition, the UV−vis absorption behavior of the copolymer solutions implied that the ground state conformations of PBZT in MSA were greatly dependent on the amorphous or the semicrystalline nature of the PEK unit, which has little or no effect on the emission properties.

Introduction

Highly fused aromatic heterocyclic rigid-rod polybenzobisazoles such as polybenzobisthiazoles (PBZTs), polybenzobisoxazoles (PBOs), and polybenzobisimidazoles (PBIs) are well known for their excellent thermal and mechanical properties[1] as well as their optical and electronic characteristics[2] and continue to captivate the research community of high-performance, heat-resistant polymers. These lyotropic liquid-crystalline polymers are, in general, prepared from heterogeneous polycondensation above the critical polymer concentration (∼4−5 wt %) in a mild acid such as poly(phosphoric acid) (PPA, 83% P_2O_5 assay) at elevated temperatures (Scheme 1).[3] Because of the limited solubility and extremely high glass transition temperatures of polybenzobisazoles, the only practical processing option has been fiber spinning directly from the polymerization mixtures. The resultant fibers displayed extremely high tensile strength and modulus after heat treatment.[4] As such, these rigid-rod polymers have played a pivotal role in the development of the concept of the molecular level reinforcement in the field of nonmetallic structural materials.[5] In addition, they have been used in advanced composite materials and protective garments.[6,7] However, their applications have been limited due to poor processability. Due to strong lateral intermolecular interactions among the rigid-rod chains, they are only soluble in strong acidic solvents such as methanesulfonic acid (MSA), trifluoromethanesulfonic acid (TFMSA), and sulfuric acid. Melt processing is practically impossible due to their high transition temperatures, which are generally higher than their decomposition temperatures, and therefore they could not simply be blended as reinforcement additives into a coil polymer melt. The only viable option to attaining molecular-level composites is solution processing in strong acidic solvents. In that case, achieving molecular level dispersion of a rigid-rod polymer in the matrix is of paramount importance in order to maximize the reinforcement efficiency. To arrive at such a state, the added amount of rigid-rod polymer should be less than its corresponding critical concentration to prevent the occurrence of microscale-to-macroscale phase separation.[8] This has restricted the concentration of the rigid-rod polymer for processing of molecular composites from solutions to considerably less than 4−5 wt %. Furthermore, with little or no strong specific interactions between the rigid-rod polymer and the coil-matrix polymer, the effect of critical concentration will undoubtedly lead to the segregation and premature precipitation of the rigid-rod polymers from the solution during vacuum-film-casting process. To circumvent such a macrophase separation problem, triblock copolymers have been developed using rigid-rod PBZT and semirigid benzazoles such as polybenzimidazole or polybenzoxazole.[9] Still, these semirigid units were only soluble in strong acidic solvents and displayed extremely high transition temperatures. An ideal molecular composite system reinforced by a rigid-rod polymer should be easy in both synthesis and fabrication. The approach of ABA triblock copolymer system to molecular composites is attractive because such a molecular composite could be in principle prepared by a one-pot synthesis process in the same reaction medium and, with the judicious choice of A-block component (coil), could be easily fabricated

* Corresponding authors. E-mail: jbbaek@chungbuk.ac.kr (J.-B.B.). Telephone: +82-43-261-2489. Fax: + 82-43-262-2380. E-mail: Loon-Seng.Tan@wpafb.af.mil (L.-S. T.). Telephone: +1-937-255-9141. Fax: + 1-937-255-9157.

† Chungbuk National University.

‡ Wright-Patterson Air Force Base.

10.1021/ma071757e CCC: $40.75
Published on Web 02/05/2008

Scheme 1 Synthesis and Structure of Polybenzobisthiazole (PBZT)

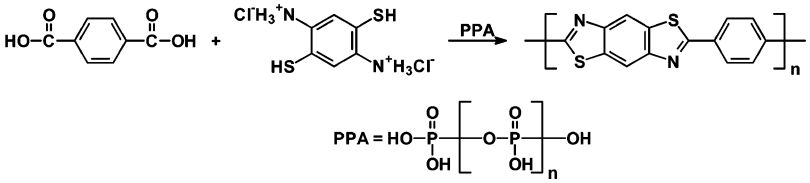

Scheme 2 Synthesis of Polyetherketones

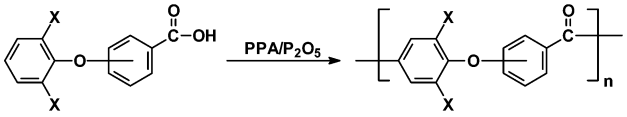

by both solution and melt processing methods. In other words, the role of the rigid-rod B-block unit in the block copolymer is to provide reinforcement and that of the coil A-block component is to promote fluidity or solubility for fabrication. A key step in the approach to an ABA triblock copolymer is the preparation of rigid-rod polybenzobisazoles end capped with appropriate reactive end groups. The groups should be reactive enough for the next step reaction in the same reaction medium. However, due to the poor solubility of even micronized terephthalic acid (TA) in PPA, the rigid-rod benzobisazole oligomers are not statistically end capped at the two monomer feed ratios when they are polymerized above the critical concentration (in lyotropic phase).[10] Thus, to afford statistically end-capped polybenzobisazoles, it is crucial to carry out homogeneous polymerization with the polymer content below its critical 4−5 wt % concentration in PPA.

In this regard, the rigid-rod B-block, which is terminated with carboxylic acid at both ends of the polybenzobisazole unit, could be obtained by adding excess amounts of terephthalic acid at below the critical concentration. The following sequence to obtain ABA triblock copolymers is to incorporate block units such as linear coils at both chain ends by addition of appropriate AB monomer for A-block units in the same reaction medium. Strong intermolecular interactions of polybenzobisazole units could be reduced by random coil A-blocks. This approach is further extended to enhance electronic and optical characteristics of the fused aromatic systems with little sacrifice to their outstanding physical properties.[11]

As a coil B-block candidate, linear polyetherketones (PEKs) are also well known as high performance engineering plastics.[12] We have developed and reported a superior reaction medium that drives the direct electrophilic substitution reaction from carboxylic acid instead of from carboxylic acid chloride as a polymer forming reaction.[13] The system consists of commercial PPA grade (PPA, 83% P_2O_5 assay), which is the same reaction medium for polybenzobisazoles. By addition of a proper amount of phosphorus pentoxide (P_2O_5) at 130 °C, the reaction condition was optimized for direct Friedel−Crafts acylation. With this synthesis protocol, very high molecular weight PEK could be afforded (Scheme 2).

By combination of the reaction conditions for both the rigid-rod polybenzobisazole and the coil PEK in the same reaction medium PPA, the preparation of ABA triblock copolymers via a simple one-pot process can be accomplished. Thus, this work reports the synthesis of a series of ABA triblock copolymers consisting of three different high performance coil polymers as A-block units and PBZTs with two different molecular weights as the B-block unit. The basic properties of the resultant materials were studied to provide a fundamental understanding of the structure−property relationship inherent to these systems and to demonstrate the improvement in the processability of the rigid-rod PBZT rendered by incorporation of melt processable coil PEK. Furthermore, optical properties of triblock copolymers in MSA solutions are also reported.

Experimental Section

Materials. All chemicals and solvents including polyphosphoric acid (PPA, assay ≥83% P_2O_5 content) and phosphorus pentoxide (P_2O_5) were purchased from Aldrich Chemical Inc. and used as received, unless otherwise specified. The AB monomers, 3- and 4-phenoxybenzoic acids for linear polyetherketones (PEKs) were purchased from Aldrich Chemical Co. They were purified by recrystallization from toluene/heptane (5/5, vol/vol) mixture to give shiny colorless needles (mp 147−148.5 and 162−164 °C, respectively).[13,14] The other AB monomer 2,6-dimethylphenoxybenzoic acid was synthesized following a modified literature procedure to afford white needles, mp 186−188 °C.[13]

Instrumentation. Elemental analysis and mass spectral analysis were performed by System Support Branch, Materials & Manufacturing Directorate, Air Force Research Laboratory, Dayton, Ohio. The melting points (mp) of all compounds were determined on a Mel-Temp melting point apparatus and are uncorrected. Intrinsic viscosities were determined using Cannon-Ubbelohde No. 200 viscometer. Flow times were recorded for methanesulfonic acid (MSA) solutions and polymer concentrations were approximately 0.5−0.1 g/dL at 30.0 ± 0.1 °C. Differential scanning calorimetry (DSC) analysis runs were performed in nitrogen with a ramping rate of 10 °C/min using a Perkin-Elmer DSC7 model. Themogravimetric analysis (TGA) was conducted in both inert atmosphere (helium) and air with a heating rate of 10 °C/min using a TA Hi-Res TGA 2950 thermogravimetric analyzer. UV−visible spectra were obtained on a Hewlett-Packard 8435 UV-Visible spectrophotometer. Photoluminescence measurements were performed with a Shimadzu RF-5301PC spectrofluorophotometer. The excitation wavelength used was the UV absorption maximum of each sample. The transmission electron microscope (TEM) employed in this work was a Philips CM-200 TEM with a LaB6 filament. The scanning electron microscope (SEM) used in this work was a Hitachi S-5200 instrument. Wide-angle X-ray diffraction (WAXS) of film were recorded with a Rigaku RU-200 diffractometer using Ni filtered Cu Kα radiation (40 kV, 100 mA, $\lambda = 0.15418$ nm). The energy minimization of structures were performed using CS Chem 3D standard computational package (Version 8.0, CambridgeSoft Corporation, Cambridge, MA 02140).

General Procedure for Carboxylic Acid-Terminated PBZT Homopolymers (1a and 1b). In a 100 mL resin flask equipped with a high torque mechanical stirrer and nitrogen inlet and outlet, 1,4-diamino-2,5-benzenedithiol dihydrochloride (4.0003 g, 16.316 mmol) and polyphosphoric acid (PPA, 80 g) were added. The mixture was stirred at room temperature for 24 h and then heated to 60 °C for 12 h with continuous stirring under dry N_2 purging. The mixture was further heated to 120 °C until the mixture became homogeneous and no further hydrochloric acid was detected at the gas outlet. Upon completion of the dehydrochlorination, the mixture was allowed to cool down to room temperature. Terephthalic acid (2.78159 g, 16.950 mmol) was added and the mixture was heated progressively (100 °C for 12h, 130 °C for 12h, 160 °C for 12h, and 180 °C for 4h). At the end of the reaction, the mixture was poured into water, and the pink transparent fibrous polymer was collected by suction filtration. The polymer was chopped with a

Scheme 3 Synthesis of Carboxylic Acid-Terminated Polybenzobisthiazoles

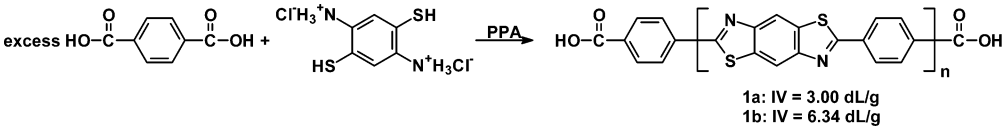

Scheme 4 Synthesis of Polyetherketone-*b*-Polybenzobisthiazole-*b*-Polyetherketone ABA Triblock Copolymers

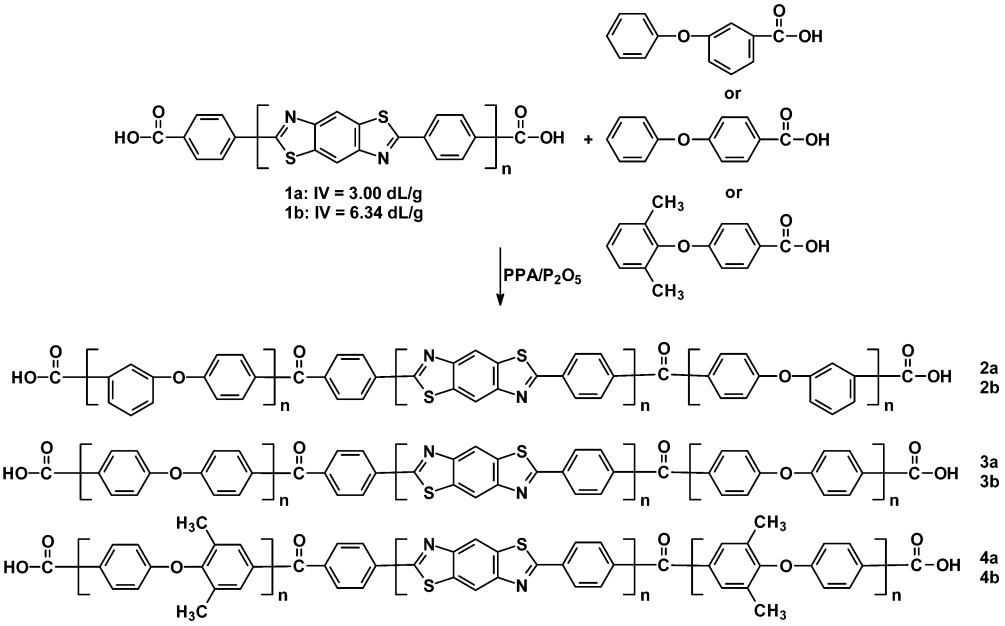

Table 1. Intrinsic Viscosity, UV−vis Absorption and Emission, and Elemental Analysis Data of Polymers

				elemental analysis		
polymer	$[\eta]^a$ (dL/g)	$\lambda_{ab}{}^b$ (nm)	λ_{em} (nm)		C (%)	H (%)
1a	3.00	443	468	calcd	63.14	2.27
				found	62.24	2.61
1b	6.34	442	468	calcd	63.14	2.27
				found	63.47	2.60
2a	3.37	401	468	calcd	74.15	3.58
				found	73.52	3.57
2b	3.88	399	469	calcd	74.15	3.58
				found	71.14	3.41
3a	2.34	423	468	calcd	74.15	3.58
				found	73.13	3.67
3b	2.81	422	468	calcd	74.15	3.58
				found	72.64	3.70
4a	2.36	409	469	calcd	75.24	4.46
				found	72.60	4.28
4b	2.52	407	468	calcd	75.24	4.46
				found	72.83	4.40

[a] Intrinsic viscosity measured in MSA at 30 ± 0.1 °C. [b] UV−vis absorption peak maxima obtained from samples dissolved in MSA. [c] Emission peak maxima obtained from samples dissolved in MSA.

Warring blender, collected by suction filtration, washed with diluted ammonium hydroxide, extracted with Soxhlet apparatus (3 days with water and 3 days with methanol), and finally dried under reduced pressure (1 mmHg) at 200 °C for 100h. The same procedure was applied for **1b**. Intrinsic viscosities of **1a** and **1b** were 3.00 and 6.34 dL/g (MSA, 30 ± 0.1 °C), respectively. For **1a** and **1b,** the calculated M_w values, on the basis of the relationship between intrinsic viscosity and number average molecular weight reported in literature for polybenzobisoxazole (PBO), were 5300 and 10 600 g/mol[15] and the UV absorption maxima in methanesunfonic acid (MSA) were at λ_{ab} = 442 nm and λ_{em} = 468 nm, respectively. Anal. Calcd for **1a** $C_{14}H_6N_2S_2$: C, 63.14%; H, 2.27%; N, 10.52%; O, 24.07%. Found: C, 62.24%; H, 2.61%; N, 9.66%; O, 22.72%. Anal. Calcd For **1b** $C_{14}H_6N_2S_2$: C, 63.14%; H, 2.27%; N, 10.52%; O, 24.07%. Found: C, 63.47%; H, 2.60%; N, 9.75%; O, 22.31%.

General Procedure for ABA Triblock Copolymers (2a and 2b). In a similar polymerization setup as described in ref 13, the B-block PBZT (1.00 g, 3.75 mmol, on the basis of the molecular weight of PBZT repeating unit) was dissolved in PPA (60 g, 83% P_2O_5 assay) at 130 °C. The mixture became homogeneous after 2−4 h at the temperature. The AB monomer (2.00 g, 9.34 mmol) for A-blocks and P_2O_5 (15.0 g, 25 wt % to the PPA) were then added and stirred at 130 °C for 48 h. The reaction condition was optimized for the direct Friedel−Crafts acylation as the polymer forming reaction from carboxylic acid instead of carboxylic acid chloride. The same workup procedure was followed as described for the carboxylic acid-terminated PBZT homopolymer. The fibrous product was finally dried under reduced pressure (1 mmHg) at 100 °C for 100 h. The intrinsic viscosity of **2a** was 3.88 dL/g (MSA, 30 ± 0.1 °C). The absorption (λ_{ab}) and emission (λ_{em}) maxima of the sample were 401 and 468 nm, respectively. Anal. Calcd for $C_{13.3}H_{7.4}N_{0.6}O_{1.4}S_{0.6}$: C, 74.15%; H, 3.58%; N, 3.02%, O, 11.63%, S, 6.90%. Found: C, 73.52%; H, 3.57%; N, 3.48%; O, 10.60%; S, 7.59%.

Results and Discussion

ABA Triblock Copolymer Synthesis. To prepare B-block component end capped carboxylic acids at both chain ends, an excess amount of micronized terephthalic acid (TA) (5.28 and 2.73 mol % excess, respectively) to 1,4-diamino-2,5-benzenedithiol (DABDT) was added to afford two different molecular weights of PBZTs. The calculated values for the average degree of polymerization (DP) of the PBZTs were 19 and 37, respectively, and the number average molecular weights (M_n's) of the polymers were 5044 g/mol and 9756 g/mol, respectively. The resultant carboxylic acid-terminated PBZTs had intrinsic viscosities of 3.00 and 6.34 dL/g (30 ± 0.1 °C in methanesulfonic acid, MSA), respectively (Scheme 3). So et al. obtained and reported a semi-empirical relationship between the intrinsic viscosity and the number average molecular weightfor PBO.[15] Because of the structural and conformational similarity between PBZT and PBO, we have used this relation

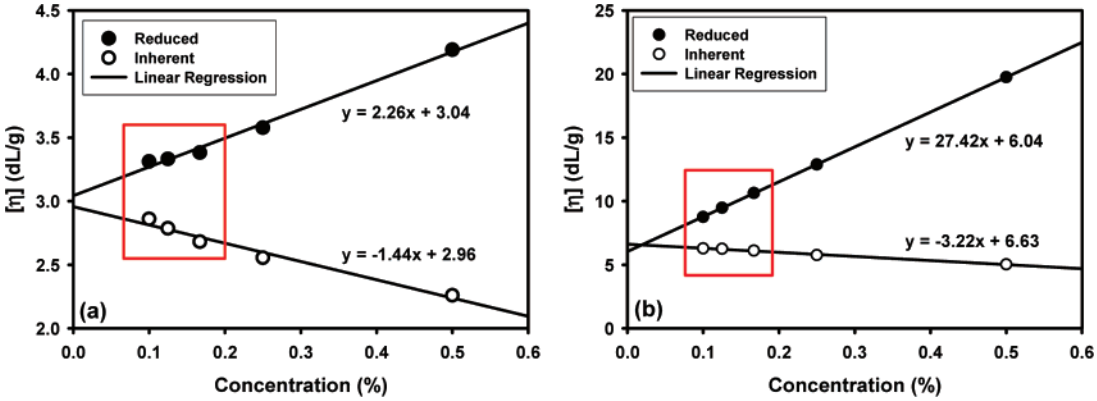

Figure 1. Solution viscosities of carboxylic acid-terminated PBZTs: (a) $[\eta] = 3.00$ dL/g; (b) $[\eta] = 6.34$ dL/g.

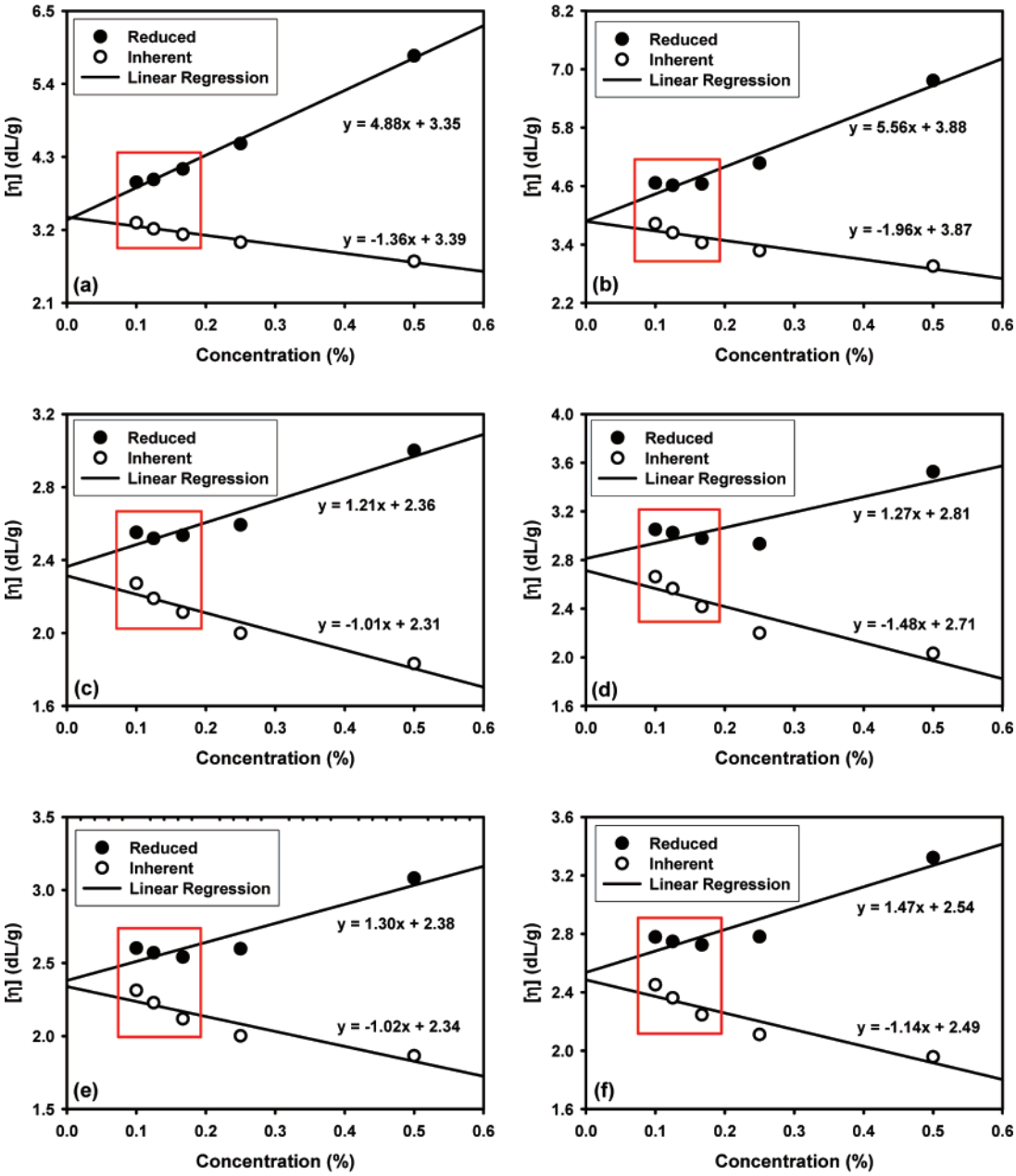

Figure 2. Solution viscosities of ABA triblock copolymers measured in MSA at 30 ± 0.1 °C: (a) **2a**; (b) **2b**; (c) **3a**; (d) **3b**; (e) **4a**; (f) **4b**.

to estimate the molecular weight and average degree of polymerization (DP) from our intrinsic viscosity data. The estimated average DP values of the PBZTs were 20 ($M_n = 5300$ g/mol) and 40 ($M_n = 10\,600$ g/mol). These values are in well agreement with theoretical values (19 and 37). For experimental consistency, the carboxylic acid-terminated PBZTs as B-block units were isolated, completely worked up, dried, and characterized. For the ABA triblock synthesis, they were first redissolved

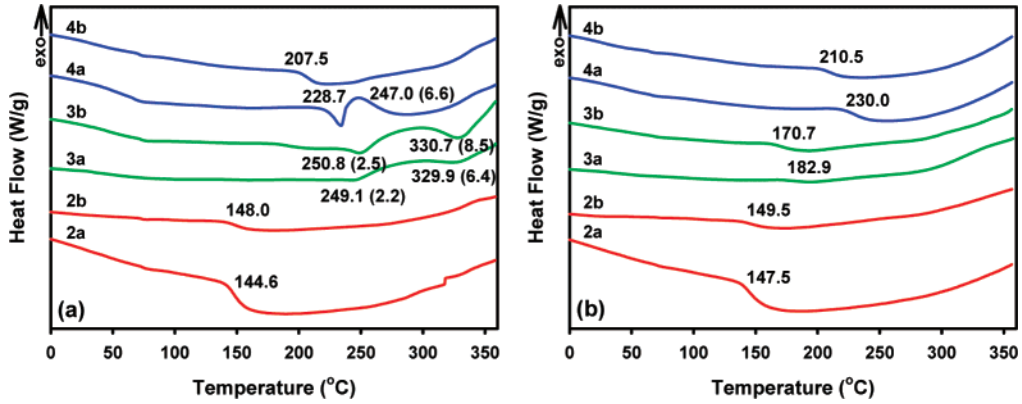

Figure 3. DSC thermograms obtained with heating rate of 10 °C/min: (a) first heating scan; (b) second heating scan.

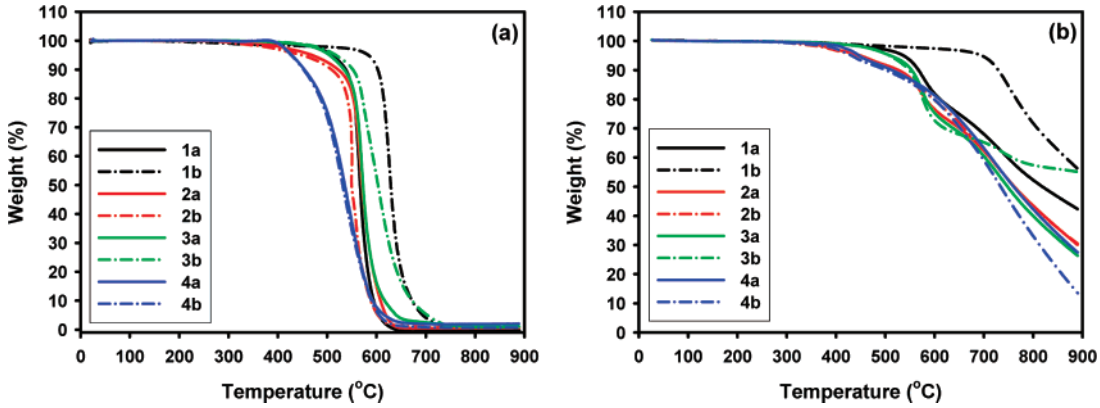

Figure 4. TGA thermograms obtained with heating rate of 10 °C/min: (a) in air; (b) in helium.

Table 2. Thermal Properties of Polymers

	DSC				TGA			
	first heating			second heating	in air		in helium	
polymer	T_g[a] (°C)	T_{m1} (°C)	T_{m2} (°C)	T_g[a] (°C)	$T_{d5\%}$[b] (°C)	char yield at 900 °C (%)	$T_{d5\%}$[b] (°C)	char yield at 900 °C (%)
1a					510	0.1	536	42.3
1b					538	0.9	695	56.2
2a	144.6			147.5	469	0.7	449	30.1
2b	148.0			149.5	448	0.7	442	30.4
3a	191.1	249.1 (2.2)	329.9 (6.4)	182.9	504	1.0	509	26.3
3b	204.8	250.8 (2.5)	330.7 (8.5)	170.7	517	1.3	507	55.1
4a	228.7			230.0	428	2.1	446	27.5
4b	207.5			210.5	427	0.8	431	13.5

[a] Inflection in baseline on DSC thermogram obtained in N_2 with a ramping rate of 10 °C/min. [b] Temperature at which 5% weight loss was recorded on TGA thermograms that were obtained with a heating rate of 10 °C/min.

in PPA. After homogeneous solutions were formed in PPA at 130 °C, the respective AB monomer was added to the polymerization vessel followed by the addition of phosphorus pentoxide. The optimal temperature and the proper amount of phosphorus pentoxide added for an efficient, direct Friedel–Crafts acylation reaction have been previously established.[13] The desired triblock copolymers were afforded as described in Scheme 4. Elemental analysis data showed a good agreement between theoretical and experimental values of the carbon and hydrogen contents of resultant products (Table 1).

Solution Properties. The PBZTs have intrinsic viscosities of 3.00 and 6.34 dL/g in MSA at 30 ± 0.1 °C. The number of carboxylic acids of the sample **1a** in the solution should be twice as that of **1b**. In comparing the solution viscosities of the samples, the general difference was clearly seen (Figure 1). The sample **1a** in MSA solution displayed relatively stronger polyelectrolyte effect as the concentration was lowered (Figure 1a), while the viscosities of the sample **1b** in the same solvent depended linearly on the concentration (Figure 1b).

In the cases of ABA triblock copolymers, their solubility was similar to that of the starting PBZTs. They displayed slightly enhanced solubility. In addition to the being soluble in MSA, trifluoromethanesulfonic acid (TFMSA), and sulfuric acid, they were also soluble in trifluoroacetic acid. The intrinsic viscosities of copolymers **2b**, **3a**, **3b**, **4a**, and **4b** are lower than those of PBZT homopolymers and the values are summarized in Table 1. All solutions in MSA displayed polyelectrolyte effects at lower concentration (Figure 2). This implied that both chain

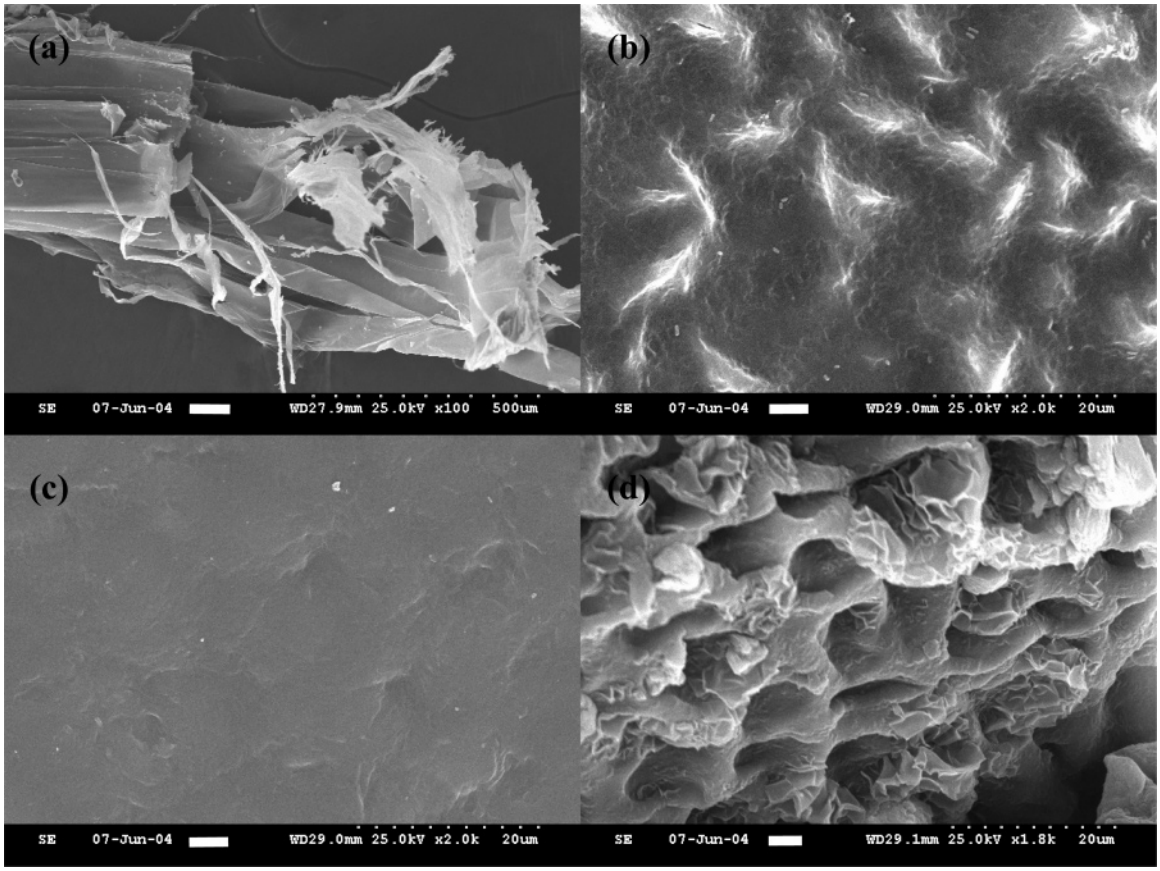

Figure 5. SEM images: (a) 1a fiber (×100, scale bar = 100 μm); (b) **2b** film (×2000, scale bar = 4 μm); (c) **3b** film (×2000, scale bar = 4 μm); (d) **3a** film (×1800, scale bar = 4 μm).

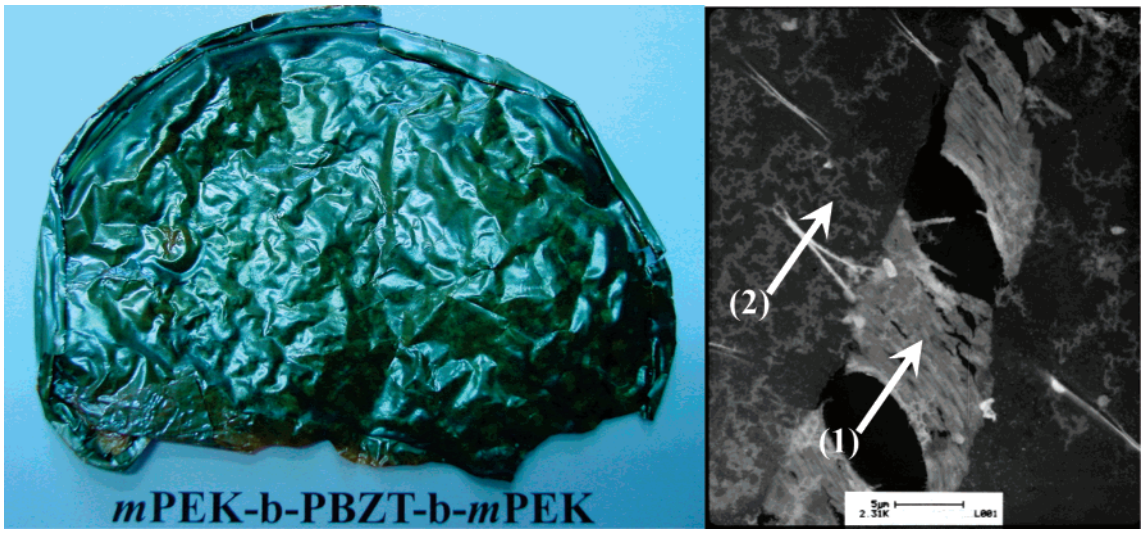

Figure 6. (a) Digital photograph of *m*PEK-*b*-PBZT-*b*-*m*PEK **2b** film. (b) TEM image of strained **2b** film (×2310, scale bar = 5 μm).

ends of triblock copolymers were carboxylic acid terminated. It was an indirect evidence that the starting PBZTs also would have been carboxylic acid terminated. The lower solution viscosity of triblock copolymers provided an indication that the incorporation of coil blocks into the rigid-rod block has indeed frustrated the alignment of the rigid-rod PBZT molecules. As a result, PBZT units in solution or melt are expected to be randomly dispersed.

Thermal Properties. The DSC samples in powder form were subjected to two cycles of heating starting from room temperature up to 360 °C and then cooling to −80 °C at a scanning rate of 10 °C/min for both heating and cooling cycles. The T_g value was taken as the midpoint of the maximum baseline shift during each heating or cooling run. As shown in Figure 3a and Table 2, the *m*PEK-*b*-PBZT-*b*-*m*PEK sample **2a** exhibited a T_g at 144.6 °C. The value is approximately 8 °C higher than that (137 °C) of the *m*PEK homopolymer.[13] The rigidity of PBZT and lower free volume in *m*PEK should have contributed to the T_g increase. Similarly, the sample **2b** displayed a T_g of 143.6 °C. As expected, both *p*PEK-*b*-PBZT-*b*-*p*PEK samples **3a** and **3b** were semicrystalline materials with two melting endotherms around 250 and 330 °C (Figure 3a). The sample

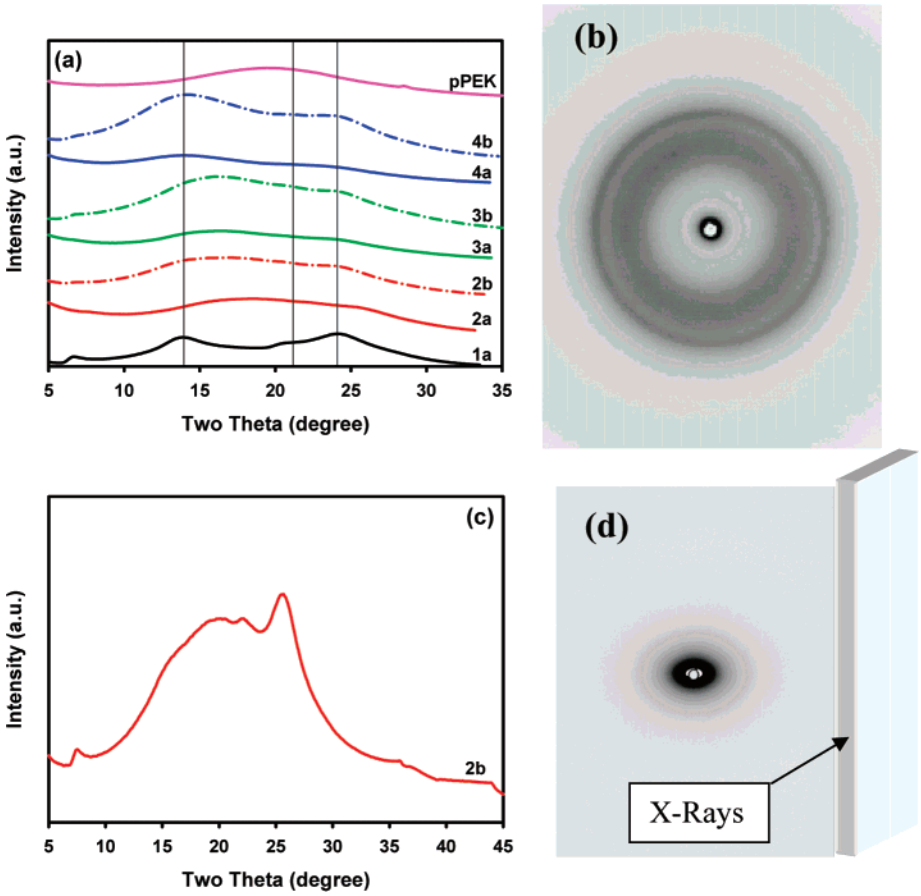

Figure 7. X-ray diffraction patterns: (a) WAXS powder *x*-*y* patterns; (a) WAXS film pattern of **2b**; (b) WAXS *x*-*y* pattern of **2b**; (c) elliptical SAXS film pattern of **2b**.

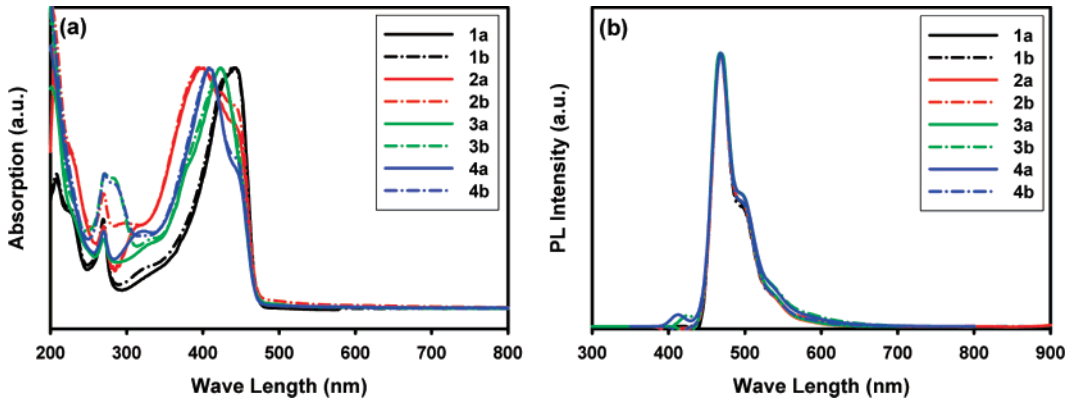

Figure 8. UV−vis absorption and emission spectra of samples: (a) absorption; (b) emission.

DiMePEK-*b*-PBZT-*b*-DiMePEK **4a** has a T_g at 228.7 °C with a quite strong peak centered at 247.0 °C. Interestingly, the T_g of sample **4b** was at 207.5 °C, whose value is approximately 20 °C lower than that of **4a**. It may be correlated to the size of PBZT molecules and the number of carboxylic acid in the system.

In the second heating scans (Figure 3b), the T_g's of the samples **2a**, **2b**, **4a**, and **4b** were increased in the range of 1.3−4.6 °C as compared to the values obtained from the first scan. This is due to an annealing effect. There were no melting endotherms detected for the samples **3a** and **3b** in the second heating scan. It must be due to the molecular motion of *p*PEK being hampered by connecting to the rigid-rod PBZT, and thus the crystallization rate was too slow to form crystals during the cooling and heating scans after melt. The samples stayed amorphous during these periods. As a result, they displayed T_g's at 182.9 and 170.7 °C, respectively. In the case of **3a** and **3b** as well as **4a** and **4b**, it was quite unexpected that the T_g decreased as the molecular weight of PBZT increased. However, the *m*PEK-*b*-PBZT-*b*-*m*PEK samples 2a and 2b behaved as expected. An explanation would invoke a couple of speculations. The first speculation would be closely related to the number of carboxylic acids in the system that could form hydrogen bonding. The lower molecular weight PBZT should contain a larger number of carboxylic acids and in turn a higher degree of hydrogen bonding. The other speculation would be the filler effect, that is, the smaller size of rigid-rod PBZT molecules would enable better filling of the larger free volume. In addition, the changes in T_g values might also be related to the molecular weight and degree of crystallinity of PEK blocks as well as the

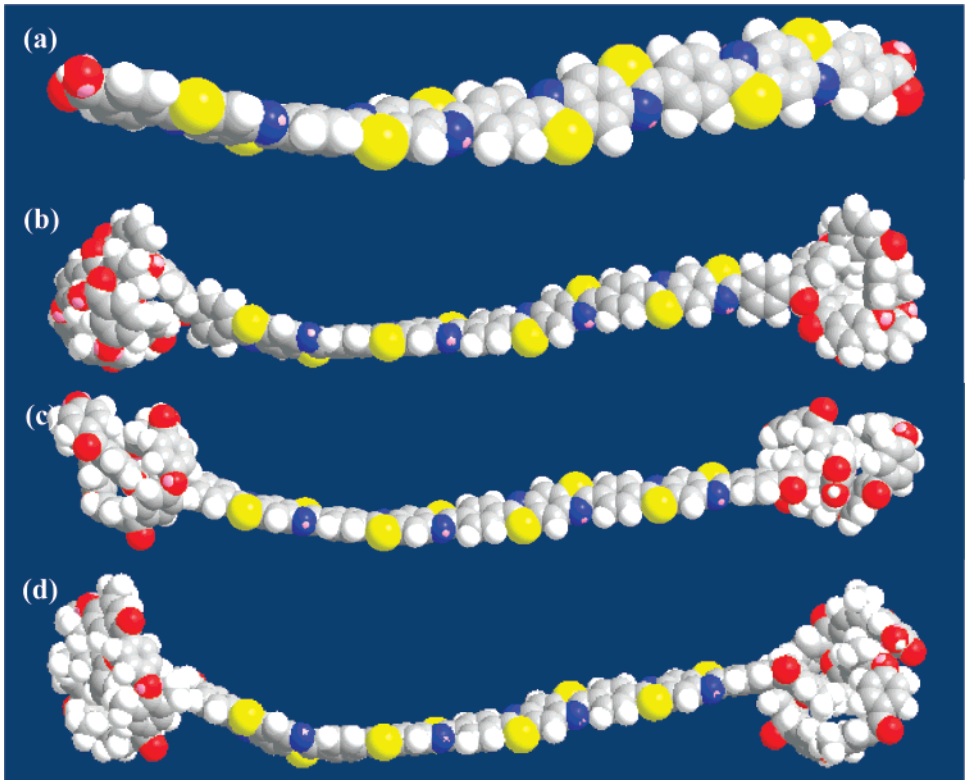

Figure 9. Schematic representation of molecular arrangement of polymer molecules: (a) PBZT; (b) *m*PEK-*b*-PBZT-*b*-*m*PEK; (c) *p*PEK-*b*-PBZT-*b*-*p*PEK; (d) DiMePEK-*b*-PBZT-*b*-DiMePEK.

conformation of triblock copolymer. Overall, these combined factors could have influenced the outcomes for the transition temperatures.

The thermogravimetic analysis (TGA) results showed that all triblock copolymer samples exhibited excellent thermal and thermooxidative stabilities with 5% weight loss temperature ranging from 427 to 517 °C in air and 431−509 °C in helium, respectively (Figure 4 and Table 2).

Scanning Electron Microscopy (SEM). The SEM image of as-spun carboxylic acid-terminated PBZT **1b** fiber resembles thin polymer sheets that were stacked together in the form of ribbon (Figure 5a). The solution-cast thin film of *m*PEK-*b*-PBZT-*b*-*m*PEK triblock copolymer **2b** was translucent and golden-brown in color (Figure 6a). It displayed very interesting SEM morphology (Figure 5b). In the surface of the film, bright fractal regions that were supposed to be PBZT aggregates were homogeneously imbedded in the dark continuous *m*PEK phase. The average size of bright domains was approximately 10 μm in length and 4 μm in width. This is a strong indication that a microphase separation has occurred during solvent evaporation and the phase-separated regions have been randomly distributed without alignment. In the case of *p*PEK-*b*-PBZT-*b*-*p*PEK triblock copolymer **3b**, the film was completely opaque and the SEM image of the film surface was uniform (Figure 5c). The difference in the morphologies of these samples could be due to the nature of PEKs, namely, *m*PEK is an amorphous polymer but *p*PEK is semicrystalline. A sample solution of **3a** in MSA was spread on a glass plate and then dipped into distilled water, resulting in the formation of a semitransparent thin film. The SEM image of this water-soaked thin film generated craterlike uniform features on its surface (Figure 5d). Apparently, they were formed during the process of coagulation in water. The average size of craters was approximately 8 μm, and there were curled ribbons surrounding them.

Transmission Electron Microscopy (TEM) Study. Generally, rigid-rod polymers have extremely high tensile strength and modulus, but they do display a few percent of elongation before breaking.[1] The TEM image of the strained **2b** film was ductile with a significant degree of elongation before break (arrow 1 in Figure 6b). Furthermore, it is apparent that microphase-separated lighter PBZT domains are homogeneously dispersed in the darker, continuous *m*PEK phase (arrow 2 in Figure 6b). Thus, the TEM observation confirms our interpretation of the corresponding SEM image (Figure 5b).

Wide-Angle X-ray Film Scattering (WAXS) and Small-angle X-ray Film Scattering (SAXS) Patterns. The WAXS pattern of PBZT **1a** showed that there was a broad but distinct ordering, as evidenced by the peaks at 3.5 and 5.5 Å (Figure 7a). Block copolymers with PBZT (intrinsic viscosity = 3.00 dL/g) **2a**, **3a**, and **4a** displayed weaker intensity as compared to those of corresponding copolymers with PBZT (intrinsic viscosity = 6.34 dL/g) **2b**, **3b**, and **4b**. The value of 3.5 Å is a typical $\pi-\pi$ distance between extended PBZT molecules. The larger PBZT units in the copolymer showed a stronger intensity. Although *p*PEK is known to be semicrystalline, the as-synthesized *p*PEK under the same reaction conditions revealed its amorphous character in the WAXS study. We have studied in detail and reported this unusual thermal relaxation behaviors of viscosity- and shear-induced strain in *p*PEK, prepared in a viscous reaction medium (PPA).[16] Similarly, the thermal behavior of triblock copolymers **3a** and **3b** is currently being studied, and the results will be reported in due course. The WAXS film diffraction pattern of the sample **2b** was considerably different from its powder pattern. There were four broad but strong equatorial reflections in the wide-angle region and a single equatorial reflection in the small-angle region (Figure 7b). Its *x*-*y* diagram is presented in Figure 7b. The *d* spacings of the equatorial reflections are 11.8, 4.4, 4.0, 3.5, and 2.4 Å. The *d*-spacing value of the second equatorial reflection (3.5 Å)

is similar to that of the PBZT homopolymer.[17] The last equatorial reflection at 11.8 Å in the small-angle region could be due to a microphase separation.

Since long range ordering was observed from WAXS film pattern, the elliptical shape of the SAXS film diffraction pattern indicated the preferential orientation of copolymer structure to be parallel to the surface of the film. Although the SAXS pattern did not show sharp equatorial reflection, there was a broad reflection observed indicating that long range ordering did exist (Figure 7d).

UV−vis Absorption and Fluorescence Study. PBZT is a well-ordered, fused aromatic, rigid-rod polymer. The polymer is highly conjugated to be optically and electrically active.[2,18] UV−vis absorption and fluorescence measurements conducted in MSA are summarized in Table 1. Absorption maxima of PBZT homopolymers **1a** and **1b** were at 443 and 442 nm, respectively, which are in the blue region. In the cases of samples containing amorphous A-block units, the absorption maxima of the block copolymers **2a** and **2b** are at 401 and 399 nm, respectively (Table 1 and Figure 8a). These absorption maxima are blue-shifted by 44 nm. Similarly, the samples **4a** and **4b** displayed absorption peak maxima centered at 409 and 407 nm, respectively (Table 1 and Figure 8a). The peaks were also blue-shifted by 35 nm. The value is lower than that of samples **2a** and **2b**. The absorption maxima of the block copolymers **3a** and **3b**, which contain semicrystalline A-block units, are at 423 and 422 nm, respectively. Compared to the PBZT homopolymers **1a** and **1b**, the peaks are blue-shifted by 20 nm, which is less than the corresponding shifts observed for samples **2a** and **2b** compared to **4a** and **4b**. However, the emission maxima are almost identical at 468−469 nm for all block copolymers (Table 1 and Figure 8b). It is noteworthy that the nature of A-block component significantly influences the ground state of PBZT conformation in MSA solution. For example, the repeating unit of *m*PEK for **2a** and **2b** should have the highest degree of freedom in molecular motion due to its doubly kinked structure at the ether-linkage and *m*-phenoxy orientation. As a result, the *m*PEK components twist the conformation of PBZT the most, resulting in a shorter effective conjugation length of the PBZT. Thus, **2a** and **2b** have the most blue-shifted value in UV−vis absorption among the samples. In the case of the samples **4a** and **4b**, the DiMePEK unit is structurally symmetrical and, therefore, is expected to possess a semicrystalline character. However, because of two methyl groups on the 2- and 6-position of the phenoxy benzene ring and a kinked structure at the ether linkage, the semicrystallinity of DiMePEK must have been greatly reduced to the point that it has a lesser degree of freedom than the *m*PEK. The *p*PEK units in the samples **3a** and **3b** are semicrystalline with the least amount of flexibility among the A components, and the UV−vis absorption of **3a** and **3b** is least affected.

To confirm the dependency of the ground state PBZT conformation on A-block components, an energy-minimization computation study was conducted with model molecules consisting of four PBZT and five PEK repeating units at both ends. The resulting space-filling molecular models showed that the twist degrees of PBZT were indeed changed with regard to the PEK components (Figure 9). The PBZT unit in the model *m*PEK-*b*-PBZT-*b*-*m*PEK was the most twisted (Figure 9b) and that in the *p*PEK-*b*-PBZT-*b*-*p*PEK was the least twisted (Figure 9c). Thus, the results agree well with the interpretation of the UV−vis absorption data.

Conclusion

In this work, we have demonstrated that PEK-*b*-PBZT-*b*-PEK triblock copolymers could be prepared as a version of molecular composites. The resultant polymeric materials were soluble in strong organic acids and had intrinsic viscosities ranging from 2.38 to 3.88 dL/g in MSA at 30 ± 0.1 °C. These triblock copolymers could be processed by both solution-casting and melt-processing techniques, which could be attributed to the PEK blocks. Good quality films were cast, and the X-ray study of these films exhibited a long range ordering indicative of microphase separation. The results showed that the PEK-*b*-PBZT-*b*-PEK triblock copolymers have more processing and fabrication options than the PBZT homopolymers and support the viability of the concept of using the rigid-rod component as a reinforcing additive and the coil component as a processing aid. Both components are bound by covalent bonds to maximize the mechanical integrity regardless of their miscibility or compatibility. In addition, their optical behavior was found to be dependent on the nature of the coil components. The ground state conformations of PBZT in MSA solutions were found to be greatly dependent on the amorphous or semicrystalline nature of the A-block unit. Irrespective of the A-block units, however, the emission maxima of sample solutions remain fixed at 468 and 469 nm. Detailed thermal, mechanical, rheological, electronic, and optical behavior as a function of PBZT loads are currently in progress. Furthermore, (hyperbranched)PEK-*b*-PBZT-*b*-(hyperbranched)PEK triblock copolymers have been synthesized, and their optical properties in basic solvents instead of protonated acidic solvents are being studied for the first time. These results will be reported separately.

Acknowledgment. We thank Shane Juhl for X-ray scattering data, Marlene Houtz for DSC and TGA data, Christopher Lyons for viscosity measurement. This project was supported by Air Force Office of Scientific Research (AFOSR) and Korea Research Foundation (KRF-2006-D00432).

References and Notes

(1) (a) Wolfe, J. E. In *Encyclopedia of Polymer Science and Technology*, 2nd ed.; Mark, H. F.; Kroschmitz, J. I., Eds.; Wiley-Interscience: New York, 1988; Vol. 11, pp 602−635 and references are there in. (b) *The Materials Science and Engineering of Rigid-Rod Polymers*; Adams, W. W., Eby, R. K., McLemore, D. E., Eds.; Materials Research Society Symposium Proceedings; Materials Research Society: Pittsburgh, PA, 1989; Vol. 134.
(2) (a) Burroughes, J. H.; Bradley, D. D. C.; Brown, A, R.; Marks, R. N.; Mackay, K.; Reiend, R. H.; Burns, P. L.; Holmes, A. B. *Nature* **1990**, *347*, 539. (b) *Handbook of Conducting Polymer*; Skotheim, T. A., Ed.; Marcel Dekker: New York, 1986, Vol. 2.
(3) So, Y.-H. *Acc. Chem. Res.* **2001**, *34*, 753.
(4) (a) Yang, H. H. *Aromatic High-Strength Fibers*; Wiley-Interscience: New York, 1989; Chapter 2. (b) Rosenberg, S.; Quarderer, G. J., Jr.; Sen, A.; Nakagawa, M.; Faley, T. L.; Serrano, M.; Teramoto, Y.; Chau, C. C. US Patent 5 294 390, 1994.
(5) Helminiak, T. E.; Benner, C. L.; Husman, G. E.; Arnold, F. E. U.S. Patent 4,207,407, 1980.
(6) Toyobo Inc. http://www.toyobo.co.jp/e/seihin/kc/pbo/menu/fra_menu_en.htm.
(7) (a) Chae, Han Gi; Kumar, Satish. *J. Appl. Polym. Sci.* **2006**, *100*, 791, and references therein. (b) So, Y. H. *Prog. Polym. Sci.* **2000**, *25*, 137.
(8) Hwang, W. F.; Wiff, D. R.; Verschoore, C. *Polym. Eng. Sci.* **1983**, *23*, 790.
(9) Tsai, T. T.; Arnold, F. E. *J. Polym. Sci., Part A: Polym. Chem.* **1989**, *27*, 2839.
(10) So, Y. H.; Heeschen, J. P.; Bell, B. *Polym. Prepr.* **1998**, *39* (1), 280.
(11) (a) Wang, S.; Wu, P.; Han, Z. *Macromolecules* **2003**, *36*, 4567. (b) Tan, L.-S.; Srinivasan, K. R.; Bai, S. J. *J. Polym. Sci., Part A: Polym. Chem.* **1997**, *35*, 1909. (c) Tan, L.-S.; Srinivasan, K. R.; Bai, S. J. *J. Polym. Sci., Part A: Polym. Chem.* **1998**, *36*, 713. (d) Tan, L.-S.; Burkett, J. L.; Simko, S. R.; Alexander, M. D., Jr. *Macromol. Rapid Commun.* **1999**, *20*, 16.

(12) (a) Fried, J. R. In *Polymer Data Handbook*; Mark, J. E., Ed.; Oxford University Press: New York, 1999; p 479. (b) Madkour, T. M. In *Polymer Data Handbook*; Mark, J. E., Ed.; Oxford University Press: New York, 1999; p 480. (c) Teasley, M. F.; Hsiao, B. S. *Macromolecules* **1996**, *29*, 6432−6441 and references therein. (d) Wood, A. S. *Mod. Plast. Int*. **1987**, 88.
(13) Baek, J.-B.; Tan, L.-S. *Polymer* **2003**, *44*, 4135.
(14) (a) Baek, J.-B.; Tan, L.-S. *Polym. Prepr*. **2002**, *43* (1), 533. (b) Baek, J.-B.; Tan, L.-S. *Polym. Prepr*. **2002**, *43* (1), 514.
(15) So, Y.-H.; Suter, U. W.; Romick, J. *Polym. Prepr*. **1999**, *40* (2), 628.
(16) Baek, J.-B.; Park, S.-Y.; Price, G. E.; Lyons, C. B.; Tan, L.-S. *Polymer* **2005**, *46*, 1543.
(17) Jenkins, S.; Jacob, K. I.; Polk, M. B.; Kumar, S.; Dang, T. D.; Arnold, F. E. *Macromolecules* **2000**, *33*, 8731.
(18) (a) Osaheni, J. A.; Jenekhe, S. A. *Macromolecules* **1993**, *26*, 4726. (b) Jenekhe, S. A.; Osaheni, J. A. *Science* **1994**, *265*, 765.

MA071757E